

Rapid precipitation in an $\text{Al}_{0.5}\text{CrFeCoNiCu}$ high entropy alloy

N. G. Jones*, K. A. Christofidou and H. J. Stone

The effect of cooling rate on the microstructural evolution of $\text{Al}_{0.5}\text{CrFeCoNiCu}$ has been studied using differential scanning calorimetry and scanning electron microscopy. As cast $\text{Al}_{0.5}\text{CrFeCoNiCu}$ contained three phases; Cr–Fe–Co–Ni solid solution dendrites, Cu rich interdendritic material and L_{12} precipitates. During cooling at rates between 10 and $50^\circ\text{C min}^{-1}$, an additional exothermic event, at $\sim 1010^\circ\text{C}$, was observed in the heat flow curves. Microstructural examination after cooling revealed the presence of two distinct populations of intragranular precipitates not present in the as cast material. Energy dispersive X-ray spectroscopy indicated that Cu rich precipitates formed within the dendrites, while a Cr–Fe–Co rich phase formed in the interdendritic constituent. Precipitation during cooling at rates approaching 1°C s^{-1} indicates that the diffusion kinetics of $\text{Al}_{0.5}\text{CrFeCoNiCu}$ is not, as previously suggested, sluggish.

Keywords: High entropy alloys, Phase transitions, Kinetics, Precipitation

This paper is part of a special issue on High entropy alloys

Introduction

Multiprincipal element high entropy alloys (HEAs), where each of the major constituents has a concentration between 5 and 35 at-%,¹ offer a new approach in materials development with practically limitless potential combinations. The term ‘HEA’ was derived from the fact that the theoretical entropy of mixing of a statistically disordered solid solution would be significantly higher than that of a conventional alloy. It was suggested that this high entropy of mixing extended the mutual solubility of different elemental species, stabilising simple structured solid solutions with respect to the formation of intermetallic compounds.¹ Studies of alloys of this type have identified a number of promising properties, including high strength,^{1–5} good wear characteristics^{6–10} and excellent corrosion resistance.^{11–13} However, while over 1400 scientific manuscripts have been published in this area to date, much of the underlying science of these materials remains under debate.

One of the key areas of research has been to establish the phase equilibria of these novel materials and determine the extent to which entropic contributions overcome enthalpic effects. The AlCrFeCoNiCu system is probably the most extensively studied and numerous different phases, both solid solution and intermetallic, have been reported.^{1,14,15} The $\text{Al}_{0.5}\text{CrFeCoNiCu}$ alloy was originally reported to contain only fcc and the related, ordered, L_{12} phases at all temperatures below the solidus.¹⁴ However, subsequent studies have identified

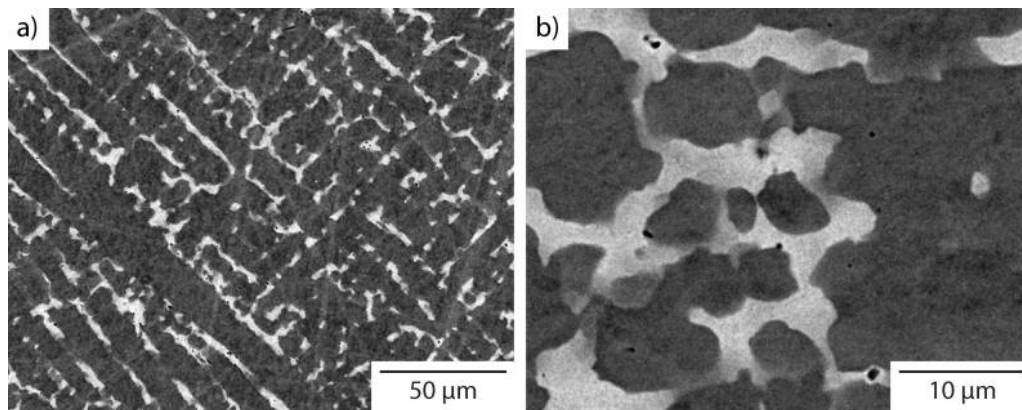
that a Ni–Al based B2 phase and a Cr–Co–Fe based σ phase precipitate in this alloy during prolonged exposures at temperatures between 700 and 1000°C .^{15,16} At higher temperatures, two fcc phases exist in equilibrium, indicating the presence of a miscibility gap in the Gibbs energy curve.¹⁷ As a result, the entropic stabilisation of these phases is reduced, increasing their susceptibility to phase decompositions at lower temperatures.^{16,17} However, the speed at which these precipitation reactions occur remains unknown. Recently, Ng *et al.*¹⁵ suggested that the diffusion kinetics of this alloy were sufficiently slow that no microstructural evolution occurred when furnace cooled from elevated heat treatment temperatures. It was proposed that the timescales required to enable a phase transformation were such that the slow cooling rates employed were equivalent to quenching a conventional alloy.

Diffusional phase transformations require the cooperative movement of different atomic species through the lattice to enable the elemental redistribution necessary to lower the Gibbs energy of the system. However, the kinetics of long range diffusion are thought to be sluggish[†] in HEAs, as a result of the complex nature of the multicomponent solid solution phases.^{1,18} It has been proposed that HEAs have highly distorted lattices, due to the different atomic radii of the constituent elements, and that this can hinder atomic movement through the structure.^{1,18} In addition, it is believed that the local configuration, bonding and energy at any given lattice site is different in an HEA,

Department of Materials Science and Metallurgy, University of Cambridge, 27 Charles Babbage Road, Cambridge CB3 0FS, UK

*Corresponding author, email ngj22@cam.ac.uk

[†] The term sluggish has been widely used in the HEA literature, without definition. Therefore, in the present work, the term is used to indicate anomalously slow diffusion when compared to other metallic systems.



1 BSEI micrographs (a 50 μm , b 10 μm) of Al_{0.5}CrFeCoNiCu in the as cast state showing a dendritic microstructure

unlike a conventional solid solution, which is dominated by a single element. Therefore, when considering substitutional diffusion through atom–vacancy interchange, it has been suggested that a moving atom may become trapped if it jumps to a lower energy site or will return to its original position if the target location is a higher energy configuration.¹⁹

Despite the large number of references to the sluggish diffusion characteristics of HEAs and the theories put forward to rationalise this behaviour, very little direct evidence exists to substantiate the claim. To date, only one study has specifically investigated this topic, using quasi-binary diffusion couples to assess the diffusion parameters of each of the subspecies in a CrMn_{0.5}FeCoNi alloy at temperatures between 900 and 1100°C.²⁰ The temperature normalised activation energies (Q/T_x , where Q is the activation energy and T_x is the melting temperature for pure metals and the solidus temperature for alloys) were found to be slightly higher in the HEA than those in either pure metals or a series of Fe–Cr–Ni alloys and this was concluded to provide evidence of the sluggish diffusion effect.²⁰ However, the normalised activation energies were not substantially greater than those of the other materials, which is perhaps surprising given the extent to which the sluggish kinetics have been alluded to. Therefore, it is clear that further work is required to establish the diffusion rates in HEAs and understand the influence of multiprincipal element solid solutions.

The present work does not attempt to make a direct assessment of the diffusion coefficients of each species in Al_{0.5}CrFeCoNiCu, but does provide new information relating to the kinetics of precipitation. In particular, it is shown that when Al_{0.5}CrFeCoNiCu is cooled from the liquid state at a constant rate, between 10 and 50°C min⁻¹, precipitates form that were not present in the as cast material, which solidified on a water cooled copper hearth. These results are in direct contrast to previous assertions and challenge the suggestion that the diffusion kinetics of this particular alloy are sluggish.^{1,14,15,21}

Experimental

A small, 40 g ingot of Al_{0.5}CrFeCoNiCu was arc melted from elemental metals, with purities of 99.95% or higher, on a water cooled Cu hearth under an inert atmosphere. The ingot was inverted and remelted a total of five times to increase the homogeneity of the final material. Differential scanning calorimetry (DSC) was conducted

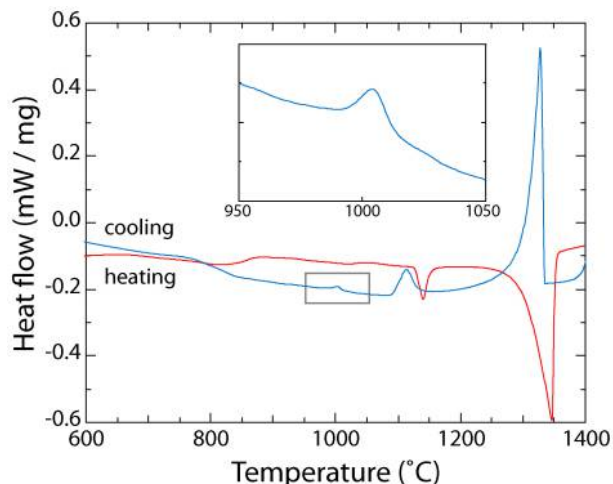
on 5 mm diameter discs using a Netzsch 404 high temperature calorimeter under flowing argon. Samples were heated at a rate of 10°C min⁻¹ to a maximum temperature of 1450°C, ~100°C above the liquidus temperature of the material, and held at this temperature for 10 min. Cooling from 1450°C was performed at nominal rates of 10, 15, 20, 30, 40 and 50°C min⁻¹, which were achieved experimentally to within $\pm 1^\circ\text{C min}^{-1}$ until a temperature of 500°C. The DSC samples were sectioned vertically and metallographically prepared using P800–P4000 grade silicon carbide paper, followed by polishing using a 0.06 μm colloidal silica solution. Microstructural characterisation was performed using backscattered electron imaging (BSEI) in a JEOL 5800 scanning electron microscope and an FEI Nova NanoSEM 450. Elemental partitioning information was obtained in the latter instrument using a Bruker XFlash 6 solid state energy dispersive X-ray (EDX) detector.

Results

The composition and microstructure of Al_{0.5}CrFeCoNiCu in the as cast state has been characterised extensively in previous publications.^{16,17} However, for completeness and ease of comparison with the results presented later, BSEI micrographs from the as cast condition are shown in Fig. 1. Following arc melting and rapid cooling on a water chilled Cu hearth, a dendritic microstructure was observed, consisting of Cr–Fe–Co–Ni solid solution dendrites (darker contrast) and a Cu rich interdendritic constituent (lighter contrast). Previous work has shown that both of these phases have an fcc crystal structure and in addition, that an L₁₂ phase precipitates within the dendrites when cooled through a solvus between 800 and 850°C.^{16,17}

A DSC thermogram showing the heat flow evolution during the heating, melting and subsequent cooling of the as cast material at 10°C min⁻¹ is shown in Fig. 2. Upon heating three distinct events were observed; a sigmoid like deviation at a temperature of ~850°C, and two endothermic peaks at ~1125 and ~1350°C. The sigmoidal deviation has been associated with the dissolution of the L₁₂ precipitates back into solution, while the two large endothermic peaks correspond to the melting of the interdendritic material and the dendrites respectively.^{16,17}

Upon cooling from a liquid state, a large exothermic peak occurred at ~1325°C, corresponding to the



2 DSC thermogram from as cast $\text{Al}_{0.5}\text{CrFeCoNiCu}$ during heating (red) and cooling (blue) at $10^\circ\text{C min}^{-1}$

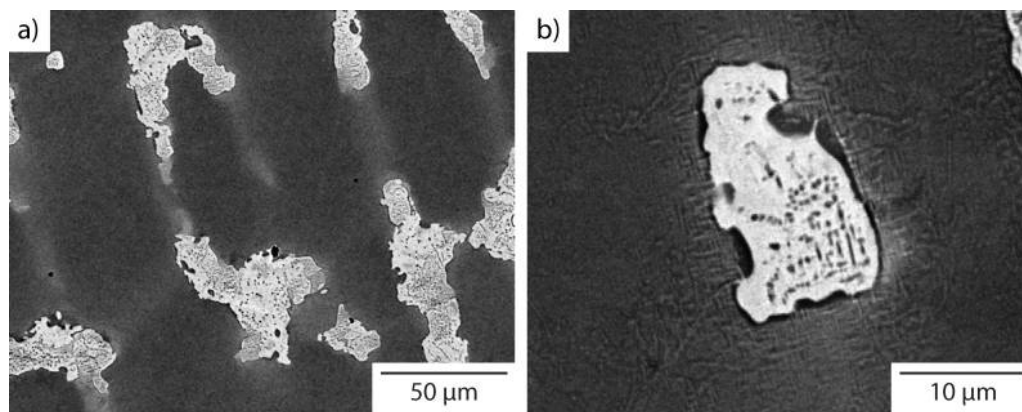
solidification of the dendrites, followed by a smaller event at $\sim 1115^\circ\text{C}$ relating to the freezing of the interdendritic material. As with the heating data, a sigmoidal deviation was observed at $\sim 815^\circ\text{C}$, which was attributed to the precipitation of the L1_2 phase. However, in contrast to the heating data, an additional exothermic event was observed in the cooling data at a temperature of $\sim 1010^\circ\text{C}$ (see inset of Fig. 2). This event suggested that the microstructural state following cooling at $10^\circ\text{C min}^{-1}$ was different from that observed in Fig. 1, which was rapidly cooled on a water chilled copper heath.

The microstructure obtained following cooling at $10^\circ\text{C min}^{-1}$ is shown in Fig. 3. As with the as cast condition, the material had a dendritic microstructure, but the slower cooling rate produced significantly coarser features than those shown in Fig. 1, for example, the size of the interdendritic regions. Critically, and in contrast to the as cast material, small precipitates, with a maximum dimension $< 4\ \mu\text{m}$, were observed within the lighter contrast interdendritic material. In addition, fine acicular precipitates were also observed within the dendrites. These are more clearly seen in the higher magnification image given in Fig. 3b. EDX elemental distribution maps, shown in Fig. 4, were obtained from an area containing both dendritic and interdendritic material. The dendrite phase, present in the top left and

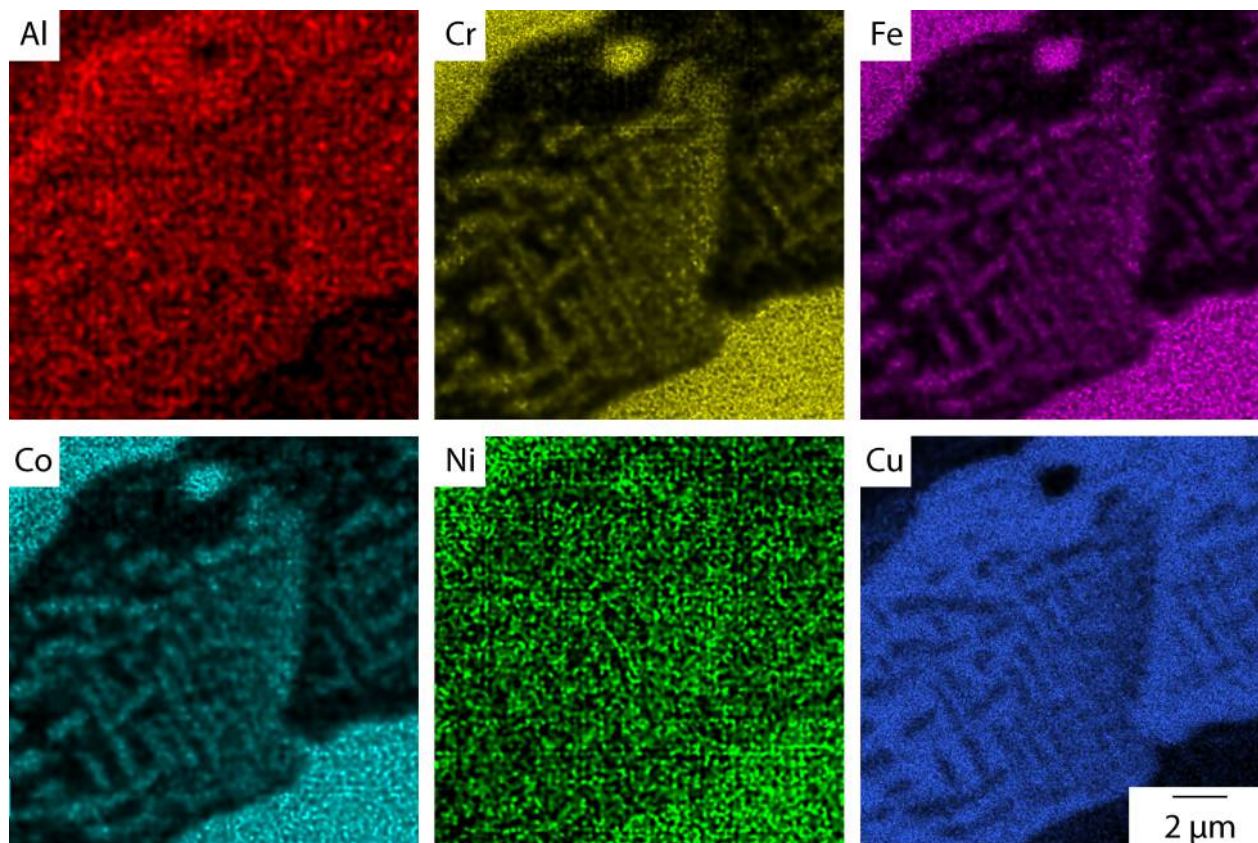
bottom right corners of the images, was rich in Cr, Fe and Co, while the interdendritic material, as shown in the centre of the image, was predominantly rich in Cu. The distribution of Ni and Al was more even between these two constituents, with Ni showing slightly higher concentrations in the dendrite regions and Al in the interdendritic material. The elemental partitioning between the dendritic and interdendritic regions is consistent with previous reports of as cast condition material.^{14,16,17}

The precipitates observed within the interdendritic material in Fig. 3 were also clearly evident in the EDX maps shown in Fig. 4. These precipitates were found to be rich in Cr, Fe and Co with extremely limited solubility for Cu. No preferential partitioning of Ni and Al could be determined from the maps obtained, suggesting an approximately even distribution of these elements. Secondary electron imaging showed that the larger circular feature within the interdendritic material at the top of the image was a shrinkage pore and that, therefore, the EDX signal corresponded to the dendrite phase beneath. However, this is a useful observation, as the contrast difference between this area and the smaller precipitates indicated that there is a compositional difference between the two features. In addition, the elemental maps shown in Fig. 4 indicated that an orientation relationship existed between the precipitates and the Cu rich interdendritic phase. The major axes of the precipitates are $\sim 90^\circ$ to each other, suggesting a strong orientation relationship with respect to the fcc parent structure.

A high magnification BSEI micrograph of the acicular precipitates present within the dendritic material is shown in Fig. 5a. A fine Widmanstätten structure of high aspect ratio precipitates was observed, all of which were less than $2\ \mu\text{m}$ in length. As with the precipitates observed within the interdendritic region, the major axes of these precipitates also appear to be at $\sim 90^\circ$ to each other, which suggested that they also have a well defined orientation relationship with the parent phase. The lighter backscattered contrast suggested that these precipitates have a greater concentration of heavier elements than the Cr–Fe–Co–Ni rich dendrite phase. An EDX map of the distribution of Cu is presented in Fig. 5b. Elevated levels of Cu were seen in formations that correlated with the precipitates shown in Fig. 5a, which is consistent with the BSEI observation.



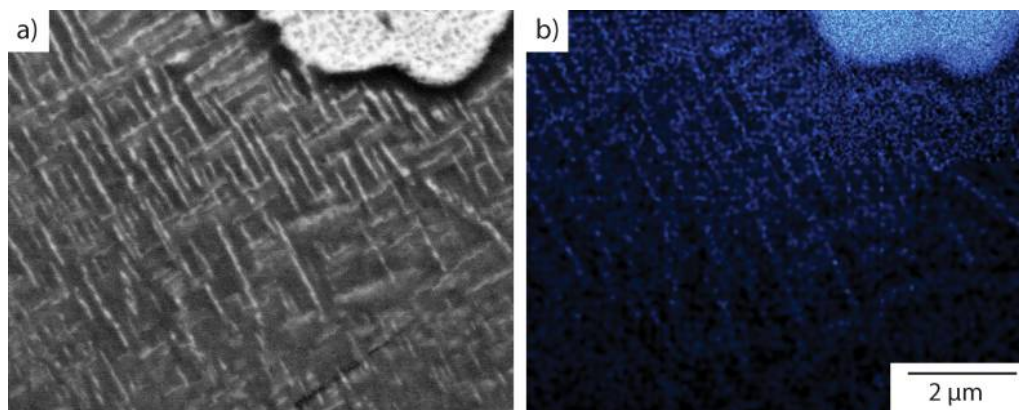
3 BSEI micrographs (a $50\ \mu\text{m}$; b $10\ \mu\text{m}$) of $\text{Al}_{0.5}\text{CrFeCoNiCu}$ cooled at $10^\circ\text{C min}^{-1}$ from the liquid state



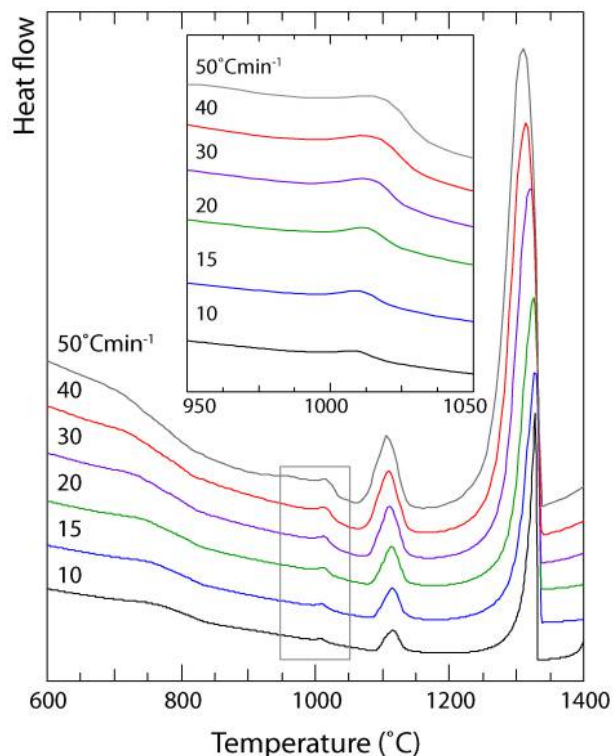
4 EDX elemental distribution maps from Al_{0.5}CrFeCoNiCu cooled at 10°C min⁻¹ showing Cr, Fe and Co rich precipitates within the interdendritic constituent

Heat flow data was also obtained from samples cooled from the liquid state in the DSC at rates of 15, 20, 30, 40 and 50°C min⁻¹. The thermograms corresponding to these experiments are shown in Fig. 6, and clearly exhibit the same exothermic event around 1010°C that was observed in Fig. 2. It is well known that changing the cooling rate alters both the shape and position of a DSC peak; faster rates result in peaks that have greater amplitude, but which are depressed further from the true transformation temperature.^{22,23} Such trends can be seen clearly for the two solidification events in Fig. 6. Therefore, it is interesting to note that the position of the peak around 1010°C increased at faster cooling rates, which can be more clearly seen in the inset of Fig. 6. Nevertheless, the presence of this peak suggested that

the precipitation of the extra phases observed in Fig. 3 occurred, even when cooling at a rate close to 1°C s⁻¹. To verify this result, the microstructure of the material cooled at 50°C min⁻¹ was examined in the electron microscope. Micrographs obtained by BSEI from the 50°C min⁻¹ sample are shown in Fig. 7, and revealed a dendritic structure similar in nature and length scale to that of the sample cooled at 10°C min⁻¹. Consistent with the microstructure shown in Fig. 3, small precipitates were observed within the interdendritic material, albeit at a slightly finer scale than those observed following cooling at 10°C min⁻¹. EDX maps, as shown in Fig. 8, indicated that the elemental partitioning was very similar to that observed in the sample cooled at 10°C min⁻¹. The dendrites were found to be rich in Cr,



5 a) BSEI of the microstructure of Al_{0.5}CrFeCoNiCu cooled at 10°C min⁻¹ showing precipitation in both the dendritic and interdendritic constituents and b) corresponding Cu EDX map indicating that the fine acicular precipitates within the dendrites are Cu rich



6 DSC thermograms illustrating the influence of cooling rate on Al_{0.5}CrFeCoNiCu

Fe and Co, while the interdendritic material was Cu based and the precipitates within this phase were rich in Cr, Fe and Co. Evidence of the Widmanstätten precipitates within the dendrites was also observed in the BSEI. However, the scale of these precipitates was too fine to enable partitioning data to be collected via EDX mapping in an SEM.

Discussion

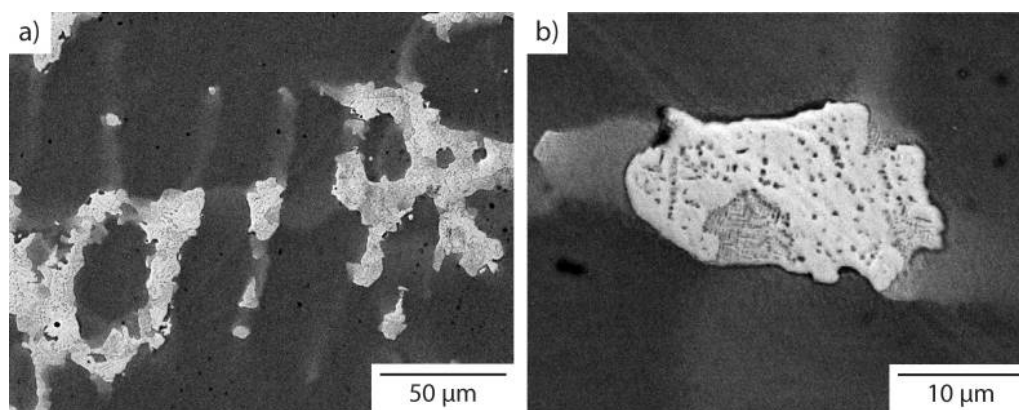
The observation of precipitates, both within the dendritic and interdendritic material following relatively fast, constant rate cooling, is highly significant, particularly given the previous claims of sluggish diffusion in this alloy. The formation of precipitates, such as those seen in Figs. 3 and 5, requires the coordinated long range diffusion of different atomic species. The fact that pronounced segregation has occurred during such a short time period clearly indicated that the diffusion

kinetics of different atomic species within Al_{0.5}CrFeCoNiCu are not slow. It could be argued that this result is unsurprising for the interdendritic regions, as this phase is predominantly Cu rich and would therefore be expected to behave as a conventional alloy. However, the same argument cannot be made for the dendritic material, where at least four elements are present in near equiatomic concentrations.

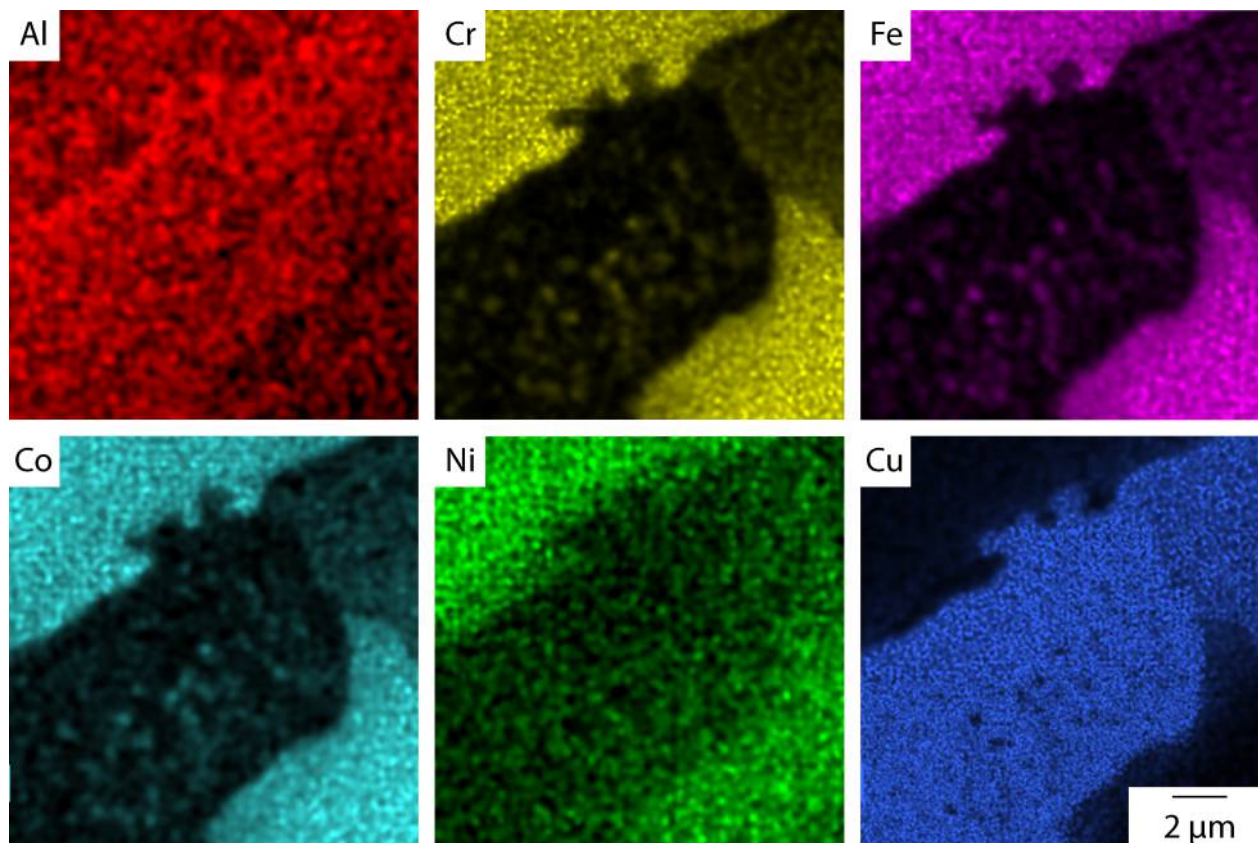
The high temperature phase equilibria of Al_{0.5}CrFeCoNiCu is known to consist of two fcc solid solutions, but at temperatures below 1000°C, it has now been established that three other phases can also exist in equilibrium; a Ni–Al based B2, a Cr–Co–Fe based σ phase and an L₁₂ phase.¹⁶ Formation of the B2 phase has been reported following extended heat treatments at temperatures between 700 and 900°C, but was not present when annealed at or above 1000°C.^{15,16} Similarly, the σ phase has been observed to form during exposures to temperatures within the range of 700–850°C, but was not present at 900°C.^{15,16} The L₁₂ phase is often found in the room temperature microstructure of this alloy, as the solid state ordering transformation appears to be quench insuppressible.¹⁷ However, it is only in equilibrium below the solvus temperature, which lies between 800 and 850°C.¹⁶

Given that the additional, exothermic event in the DSC thermograms occurred just above 1000°C (Figs. 2 and 6), and that the B2 phase has been reported to form following a 1 h heat treatment at 900°C,¹⁵ it might be expected that the precipitates observed in Fig. 3 would correspond to this phase. However, neither of the two precipitate phases observed in the current study have a chemistry remotely similar to that previously reported for the B2 phase.¹⁶ In fact, the precipitates within the interdendritic region have a chemistry that is closer to that reported for the σ phase following 1000 h exposures and therefore, presumably at equilibrium.¹⁶ Yet, it seems unlikely that the intragranular precipitates observed within the interdendritic regions are σ , since this phase has a highly complex structure and is more commonly observed to form along grain boundaries.^{24–26} In addition, previous studies of duplex stainless steels have demonstrated that cooling rates $\geq 15^\circ\text{C min}^{-1}$ are sufficient to suppress the formation of σ ,^{27–29} and nearly all of the rates considered in the present work were above this value.

High aspect ratio Widmanstätten plates have previously been observed to form within the similar composition fcc matrices of Al_{0.5}CrFeCoNiCu²¹ and



7 BSEI micrographs (a 50 μm , b 10 μm) of Al_{0.5}CrFeCoNiCu cooled at 50°C min⁻¹ from the liquid state



8 EDX elemental distribution maps from material cooled at $50^{\circ}\text{C min}^{-1}$ showing Cr, Fe and Co rich precipitates within the interdendritic constituent

Al_{0.3}CrFeCoNiCu_{0.5}³⁰ following furnace cooling from 1100°C . High resolution transmission electron microscopy has shown these plates to have elevated Cu contents with an fcc structure. In addition, Cu rich precipitates have been reported to occur in the dendritic regions of Al_{0.5}CrFeCoNiCu following long duration exposures at 850°C . These precipitates were believed to be the same phase as the interdendritic constituent.¹⁶ The observation of these two distinct precipitate populations may be rationalised through consideration of the phase equilibria and governing thermodynamics.

The Gibbs energy curve for this alloy is known to contain a miscibility gap,¹⁷ and the equilibrium compositions of the dendritic and interdendritic constituents show a significant divergence between their values at 1000°C , where they are the only stable phases, to 850°C , where four phases are in equilibrium.¹⁶ Therefore, it is unsurprising that, when rapidly cooled, the solubility limit for certain species in both of the solidification phases may be reached and that intragranular precipitation can occur. The miscibility gap in this alloy provides the potential for each of the supersaturated metastable solidification phases to separate, forming precipitates of the other thermodynamically stable phase within itself. If the driving force for such precipitation is related to the level of supersaturation in the parent solid solutions, then the behaviour of the corresponding DSC peak with respect to cooling rate can be rationalised. Slower cooling rates enable each element to diffuse greater distances, thereby reducing the levels of supersaturation in each parent phase. This reduced supersaturation lowers the Gibbs energy driving precipitation and, as a

result, the critical temperature at which the saturation limits were reached would decrease with cooling rate, depressing the onset of precipitation. Precipitates formed in this manner would exhibit a distinct orientation relationship with the parent structure that, in cubic materials, is likely to promote growth along the $\langle 100 \rangle$ due to elastic anisotropy,³¹ as seen in Al_{0.3}CrFeCoNiCu_{0.5}.³⁰ Clearly, this hypothesis is speculative at present and the crystallography of the precipitates needs to be confirmed using transmission electron microscopy. Nevertheless, the formation of precipitates in Al_{0.5}CrFeCoNiCu, when cooled at rates up to $50^{\circ}\text{C min}^{-1}$ from the liquid state, requires long range diffusion and, contrary to previous suggestions, demonstrates that the kinetics of this alloy can not be considered anomalously sluggish.

Conclusions

The microstructure of an arc melted Al_{0.5}CrFeCoNiCu high entropy alloy has been characterised using scanning electron microscopy following cooling from the liquid state at rates between 10 and $50^{\circ}\text{C min}^{-1}$. These microstructures were compared to that of the as cast material, which solidified rapidly on a water cooled Cu hearth. The as cast material, which has been characterised previously,^{16,17} contained three phases: a Cr–Fe–Co–Ni solid solution dendrite phase, Cu rich interdendritic material and L₁₂ precipitates that form when cooled through a solvus temperature between 850 and 800°C .

DSC identified exothermic events associated with solidification of the dendritic and interdendritic constituents as well as the precipitation of the L₁₂ phase. In

addition, an extra exothermic event was observed around 1010°C in the thermograms recorded from the samples cooled between 10 and 50°C min⁻¹. Microstructural examination identified the formation of new precipitates in both the dendritic and interdendritic regions. The precipitates within the dendrites were extremely fine and had an acicular morphology. EDX analysis suggested that these precipitates were slightly enriched in Cu compared with the surrounding matrix. Within the interdendritic regions, slightly coarser acicular precipitates were observed, rich in Cr, Fe and Co, but depleted in Cu. While the crystal structures of these precipitates were not established, their formation during cooling at rates approaching 1°C s⁻¹ demonstrates that the diffusion kinetics in this alloy are not, as previously reported, sluggish.

Acknowledgements

The authors would like to acknowledge support from the EPSRC/Rolls-Royce Strategic Partnership under EP/H500375/1, EP/M005607/1 (NGJ and HJS) and EP/H022309/1 (KAC).

References

- J. Yeh, S. Chen, S. Lin, J. Gan, T. Chin, T. Shun, C. Tsau and S. Chang: 'Nanostructured high-entropy alloys with multiple principal elements: novel alloy design concepts and outcomes', *Adv. Eng. Mater.*, 2004, **6**, (5), 299–303.
- O. N. Senkov, G. B. Wilks, J. M. Scott and D. B. Miracle: 'Mechanical properties of Nb₂₅Mo₂₅Ta₂₅W₂₅ and V₂₀Nb₂₀Mo₂₀Ta₂₀W₂₀ refractory high entropy alloys', *Intermetallics*, 2011, **19**, (5), 698–706.
- Y. J. Zhou, Y. Zhang, Y. L. Wang and G. L. Chen: 'Solid solution alloys of AlCoCrFeNiTi_x with excellent room-temperature mechanical properties', *Appl. Phys. Lett.*, 2007, **90**, (18), 181904.
- F. J. Wang and Y. Zhang: 'Effect of Co addition on crystal structure and mechanical properties of Ti_{0.5}CrFeNiAlCo high entropy alloy', *Mater. Sci. Eng. A*, 2008, **A496**, (1–2), 214–216.
- O. N. Senkov, C. Woodward and D. B. Miracle: 'Microstructure and properties of aluminum-containing refractory high-entropy alloys', *JOM*, 2014, **66**, (10), 2030–2042.
- M.-H. Chuang, M.-H. Tsai, W.-R. Wang, S.-J. Lin and J.-W. Yeh: 'Microstructure and wear behavior of Al_xCo_{1.5}CrFeNi_{1.5}Ti_y high-entropy alloys', *Acta Mater.*, 2011, **59**, (16), 6308–6317.
- C. Y. Hsu, J. W. Yeh, S. K. Chen and T. T. Shun: 'Wear resistance and high-temperature compression strength of Fcc CuCoNiCr Al_{0.5}Fe alloy with boron addition', *Metall. Mater. Trans. A*, 2004, **35A**, (5), 1465–1469.
- S.-T. Chen, W.-Y. Tang, Y.-F. Kuo, S.-Y. Chen, C.-H. Tsau, T.-T. Shun and J.-W. Yeh: 'Microstructure and properties of age-hardenable Al_xCrFe_{1.5}MnNi_{0.5} alloys', *Mater. Sci. Eng. A*, 2010, **A527**, (21–22), 5818–5825.
- C.-Y. Hsu, T.-S. Sheu, J.-W. Yeh and S.-K. Chen: 'Effect of iron content on wear behavior of AlCoCrFe_xMo_{0.5}Ni high-entropy alloys', *Wear*, 2010, **268**, (5–6), 653–659.
- P. K. Huang, J. W. Yeh, T. T. Shun and S. K. Chen: 'Multi-principal-element alloys with improved oxidation and wear resistance for thermal spray coating', *Adv. Eng. Mater.*, 2004, **6**, (12), 74–78.
- Y. Chen, T. Duval, U. Hung, J. Yeh and H. Shih: 'Microstructure and electrochemical properties of high entropy alloys – a comparison with type-304 stainless steel', *Corros. Sci.*, 2005, **47**, (9), 2257–2279.
- Y. Chen, U. Hong, H. Shih, J. Yeh and T. Duval: 'Electrochemical kinetics of the high entropy alloys in aqueous environments – a comparison with type 304 stainless steel', *Corros. Sci.*, 2005, **47**, (11), 2679–2699.
- Y. Hsu, W. Chiang and J. Wu: 'Corrosion behavior of FeCoNiCrCu_x high-entropy alloys in 3.5% sodium chloride solution', *Mater. Chem. Phys.*, 2005, **92**, (1), 112–117.
- C. Tong, Y. Chen, S. Chen, J. Yeh, T. Shun, C. Tsau, S. Lin and S. Chang: 'Microstructure characterization of Al_xCoCrCuFeNi high-entropy alloy system with multiprincipal elements', *Metall. Mater. Trans. A*, 2005, **36A**, (4), 881–893.
- C. Ng, S. Guo, J. Luan, S. Shi and C. T. Liu: 'Entropy-driven phase stability and slow diffusion kinetics in an Al_{0.5}CoCrCuFeNi high entropy alloy', *Intermetallics*, 2012, **31**, 165–172.
- N. G. Jones, A. Frezza and H. J. Stone: 'Phase equilibria of an Al_{0.5}CrFeCoNiCu high entropy alloy', *Mater. Sci. Eng. A*, 2014, **A615**, 214–221.
- N. G. Jones, J. W. Aveson, A. Bhowmik, B. D. Conduit and H. J. Stone: 'On the entropic stabilisation of an Al_{0.5}CrFeCoNiCu high entropy alloy', *Intermetallics*, 2014, **54**, 148–153.
- J.-W. Yeh: 'Recent progress in high-entropy alloys', *Ann. Chim. – Sci. Mater.*, 2006, **31**, (6), 633–648.
- M.-H. Tsai and J.-W. Yeh: 'High-entropy alloys: a critical review', *Mater. Res. Lett.*, 2014, **2**, (3), 107–123.
- K. Y. Tsai, M. H. Tsai and J. W. Yeh: 'Sluggish diffusion in Co–Cr–Fe–Mn–Ni high-entropy alloys', *Acta Mater.*, 2013, **61**, (13), 4887–4897.
- C.-W. Tsai, Y.-L. Chen, M.-H. Tsai, J.-W. Yeh, T.-T. Shun and S.-K. Chen: 'Deformation and annealing behaviors of high-entropy alloy Al_{0.5}CoCrCuFeNi', *J. Alloys Compd.*, 2009, **486**, (1–2), 427–435.
- W. J. Boettinger, U. R. Kattner, K. W. Moon and J. H. Perepezko: 'DTA and heat-flux DSC measurements of alloy melting and freezing', 960-15; 2006, Gaithersburg, MD, NIST.
- G. Höhne, W. F. Hemminger and H.-J. Flammershei: 'Differential scanning calorimetry'; 2003, Berlin, Springer.
- C. M. F. Rae and R. C. Reed: 'The precipitation of topologically close-packed phases in rhenium-containing superalloys', *Acta Mater.*, 2001, **49**, (19), 4113–4125.
- E. O. Hall and S. H. Algie: 'The sigma phase', *Metall. Rev.*, 1966, **11**, (1), 61–88.
- A. K. Sinha: 'Topologically close-packed structures of transition-metal alloys', *Prog. Mater. Sci.*, 1972, **15**, (2), 79.
- T. H. Chen and J. R. Yang: 'Effects of solution treatment and continuous cooling on sigma-phase precipitation in a 2205 duplex stainless steel', *Mater. Sci. Eng. A*, 2001, **A311**, (1–2), 28–41.
- L. H. Chiu, W. C. Hsieh, and C. H. Wu: 'Cooling rate effect on vacuum brazed joint properties for 2205 duplex stainless steels', *Mater. Sci. Eng. A*, 2003, **A354**, (1–2), 82–91.
- H. Sieurin and R. Sandström: 'Sigma phase precipitation in duplex stainless steel 2205', *Mater. Sci. Eng. A*, 2007, **A444**, (1–2), 271–276.
- M.-H. Tsai, H. Yuan, G. Cheng, W. Xu, K.-Y. Tsai, C.-W. Tsai, W. W. Jian, C.-C. Juan, W.-J. Shen, M.-H. Chuang, J.-W. Yeh and Y. T. Zhu: 'Morphology, structure and composition of precipitates in Al_{0.5}CoCrCu_{0.5}FeNi high-entropy alloy', *Intermetallics*, 2013, **32**, 329–336.
- J. F. Nye: 'Physical properties of crystals'; 1957, Oxford, Oxford University Press.